Journal of Power Sources 208 (2012) 159–164

Contents lists available at SciVerse ScienceDirect

Journal of Power Sources

journal homepage: www.elsevier.com/locate/jpowsour

Studies on palladium coated titanium foams cathode for Mg–H_2O_2 fuel cells

Chaozhu Shu[a,b,c], Erdong Wang[a,b], Luhua Jiang[a,b], Qiwen Tang[a,b,c], Gongquan Sun[a,b,*]

[a] Fuel Cell Division, Dalian National Laboratory for Clean Energy, Dalian 116023, China
[b] Dalian Institute of Chemical Physics, Chinese Academy of Science, Dalian 116023, China
[c] Graduate University of the Chinese Academy of Science, Beijing 100039, China

ARTICLE INFO

Article history:
Received 25 October 2011
Received in revised form
27 December 2011
Accepted 26 January 2012
Available online 4 February 2012

Keywords:
Fuel cell
Magnesium
Hydrogen peroxide
Palladium
Titanium

ABSTRACT

The corrosion resistance of several cathode substrates (titanium foam, nickel foam, and silver coated nickel foam) of magnesium–hydrogen peroxide (Mg–H_2O_2) fuel cells is studied. Titanium foam is found to be the most corrosion-resistant, i.e., the corrosion current density of titanium foam is six orders of magnitude lower than that of nickel or Ag–Ni. Palladium catalyzed titanium foam as a cathode for the Mg–H_2O_2 fuel cell is prepared by electrodepositing palladium onto the titanium foam substrate. The corrosion resistance of prepared palladium coated titanium is compared with that of titanium foam, nickel foam, and silver coated nickel foam. The structure, morphology and composition of the Pd/Ti are characterized by SEM, EDS, XRD techniques. The influence of the concentration of hydrogen peroxide, sulfuric acid and operation temperature on the performance of Mg–H_2O_2 fuel cells with the Pd/Ti cathode is studied systematically. The stability of the Mg–H_2O_2 fuel cell with the Pd/Ti as the cathode is tested and the result shows that Pd/Ti is a promising cathode material for Mg–H_2O_2 fuel cells.

1. Introduction

Recently the exploration of deep ocean gained highly attention due to the rich ocean resources, such as biology, oil and gas [1–3]. Numerous equipments powered by electricity have been used for undersea application. As a result, power sources with high energy density and environmental adaptability are extremely required. Among the various power sources, the magnesium–hydrogen peroxide fuel cell (Mg–H_2O_2 fuel cell) is a promising candidate [4,5].

Mg–H_2O_2 fuel cell, as an electrochemical system with high specific energy, is capable of converting chemical energy stored in magnesium and hydrogen peroxide to electrical energy. The half-cell and overall reactions and the standard potentials for the Mg–H_2O_2 fuel cell are shown in Eq. (1)–(3).

$$\text{Anode reaction}: Mg \rightarrow Mg^{2+} + 2e^- \quad -2.37\,V(\text{vsSHE}) \tag{1}$$

$$\text{Cathode reaction}: H_2O_2 + 2H^+ + 2e^- \rightarrow 2H_2O \quad 1.78\,V(\text{vsSHE}) \tag{2}$$

$$\text{Overall reaction}: Mg + H_2O_2 + 2H^+ \rightarrow Mg^{2+} + 2H_2O \quad 4.15\,V(\text{vsSHE}) \tag{3}$$

The theoretical voltage of a Mg–H_2O_2 fuel cell is 4.15 V (in acidic media), which is higher than the power sources in use currently, such as aluminum–silver oxide (Al/AgO) or aluminum–hydrogen peroxide (Al–H_2O_2) fuel cells [6]. Besides, the Mg–H_2O_2 fuel cell possesses the advantages of environmental benign and low costs. However, both the performance and stability of the Mg–H_2O_2 fuel cell still need to be improved before its commercialization. The cathodic catalytic material of the Mg–H_2O_2 fuel cell, as a key component, predominantly determines the performance and stability of Mg–H_2O_2 fuel cells. Extensive studies on both the cathode, especially the catalysts for hydrogen peroxide reduction reaction, and the substrates have been explored [7–9]. Bessette et al. [10] studied an Ir_2O_3–Pd core–shell catalyst prepared by the electrodeposition method, and then supported the catalyst on active carbon, used as the cathode for an Al–H_2O_2 fuel cell. It was found that the initial and long-term performance of the Al–H_2O_2 fuel cell was improved significantly. Based on the above study, Bessette et al. [11] further fabricated a microfiber carbon electrode (MCE) covered by stable Pd/Ir clusters using a textile science flocking technique. A maximum power density of 90 mW cm^{-2} was obtained by increasing the Pd/Ir loading in the cathode to 10 mg cm^{-2}. Medeiros and Dow [12] studied comparatively the carbon and nickel foil substrate with Pd/Ir catalyst in a Mg–H_2O_2 fuel cell. The cell voltages of 1.3 V and 1.5 V were obtained with the nickel foil and carbon substrate catalyzed by Pd/Ir catalyst at 25 mA cm^{-2}, respectively. Previously, our group prepared a Pd/Ag catalyzed nickel foam cathode for the Mg–H_2O_2 fuel cell, and a maximum power density of 138 mW cm^{-2} was obtained at 50 °C [13].

* Corresponding author at: Dalian Institute of Chemical Physics, Chinese Academy of Sciences, Dalian 116023, China. Tel.: +86 411 84379063; fax: +86 411 84379063.
E-mail address: gqsun@dicp.ac.cn (G. Sun).

0378-7753/$ – see front matter.
doi:10.1016/j.jpowsour.2012.01.140

As of a Mg–H_2O_2 fuel cell, to achieve a better performance and stability, besides a high catalytic activity of the catalyst toward the hydrogen peroxide reduction reaction, the properties of the substrate material for cathodic catalysts should also be considered. A good substrate in an acidic Mg–H_2O_2 fuel cell must have the following properties: (i) high electric conductivity, (ii) strong corrosion-resistance to seawater and acid, (iii) a porous structure. Unfortunately, the traditional electrode materials, such as nickel and carbon, can hardly meet the above requirements. Although nickel foam is a good conductor, and often used as the current-collector of many batteries, it seems unsuitable to be as the cathode material because of the strong corrosion in acidic media [14]. Carbon is known as its excellent corrosive resistance in different media. However, it is of challenge to prepare a carbon-based substrate with both high electronic conductivity and good mechanical property [15]. Titanium, as a metal could provide high electric conductivity, strong corrosion resistance, and good mechanical strength [16–18] is a very prospective material as the cathode substrate for Mg–H_2O_2 fuel cells.

In this paper, a Pd coated titanium foam cathode was prepared via electrodepositing Pd onto a porous titanium foam substrate. The morphology and composition of the Pd catalyzed titanium foam were characterized by scanning electron microscopy (SEM), energy dispersive X-ray spectroscopy (EDS), and X-ray diffraction (XRD). The effects of operation temperatures, hydrogen peroxide concentrations, sulfuric acid concentrations on the cell performance were investigated systematically.

2. Experimental

2.1. Materials

All chemicals used in this study were of reagent-grade quality and used as received from J&K Chemical Ltd. without purification further. All solutions were prepared using deionized water. The anode is AZ61 magnesium alloy.

2.2. Electrode preparation

The titanium foam used in this work was purchased from Dechen Ltd. with a thickness of 0.7 mm and pore size and porosity is 100 μm and 40%, respectively. The electrical conductivity of Ti is 2.22×10^6 S m^{-1}. The nickel foam was purchased from Shenzhen Rolinsia Power Materials Ltd. with a thickness of 1.0 mm and a pore density of 110 ppi. The silver coated nickel foam substrate was prepared via direct electrodepositing silver onto the nickel foam with 50 g L^{-1} of $KAg(CN)_2$ by controlling the electrolyte composition and deposition conditions. Electrodeposition was carried out at a current density of 5 mA cm^{-2} at room temperature. The electrodeposition time was controlled to obtain a coating thickness of about 1 μm. After deposition, a gray metal silver film was formed on the surface of nickel foam substrate.

Before eletrodeposition of Pd, the titanium foam was treated as follows to obtain a fresh surface. First, the titanium foam was washed with acetone to remove the grease on the titanium surface. Then, the titanium foam was etched at 90 °C in the mixture of hydrochloric acid and oxalic acid, followed by the activation of the titanium surface in the mixture of hydrofluoric acid and nitric acid. The electrodeposition of Pd was performed in an aqueous solution of 0.025 M $PdCl_2$ and 0.1 M HCl at a current density of 2 mA cm^{-2} at room temperature. The Pd loading on titanium foam was 1 mg cm^{-2} by controlling the electrodeposition time.

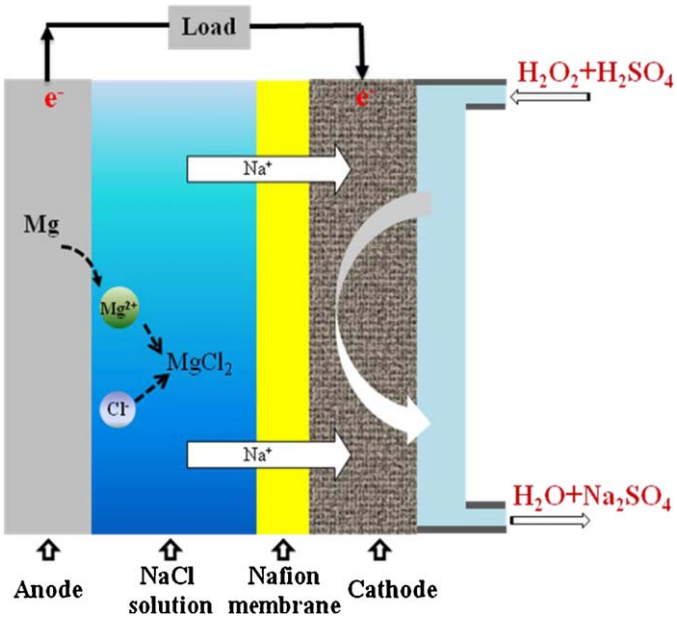

Fig. 1. The schematic structure of a Mg–H_2O_2 fuel cell.

2.3. Potentiodynamic tests

The polarization curves of the nickel foam, the silver coated nickel foam, the titanium foam and the palladium coated titanium foam were tested in 0.5 M H_2SO_4 by the electrochemical work station (solartron 1287). The reference electrode was a saturated calomel electrode (SCE). The counter electrode was a platinum foil. The scan rate was 1 mV s^{-1}. All tests were carried out at room temperature.

2.4. Physical characterizations

The morphology of the substrate and the cathode were obtained using a JEOL T-300 SEM system. Energy dispersive X-ray spectroscopy (EDS) analysis of titanium foam and Pd catalyzed titanium foam was carried out on a FEI Quanta 200F scanning electron microscope equipped with an energy dispersive spectrometer, the accelerating voltage were 20 kV. X-ray diffraction (XRD) patterns of the titanium foam and the Pd catalyzed titanium foam were recorded on a Rigaku D/max-2400 X-ray diffractometer using Cu Kα radiation. The tube voltage and the tube current were maintained at 40 kV and 100 mA, respectively. The scan rate was 5° min^{-1} and the step size was 0.02°.

2.5. Mg–H_2O_2 fuel cell tests

The performance and the stability tests of the Mg–H_2O_2 fuel cell were performed on a homemade cell using a fuel cell test system (Arbin Instrument Corp.). The schematic structure of the Mg–H_2O_2 fuel cell is shown in Fig. 1. The active area of the electrode was 2 cm × 5 cm. Nafion 115 membrane was put on the surface of the prepared Pd-catalyzed titanium cathode. The distance between the magnesium anode and the membrane was 1 mm. The cell test was carried out by feeding hydrogen peroxide and sulfuric acid solution in cathode. Simultaneously, an aqueous sodium chloride solution was pumped into the cell as the electrolyte. The flow rates of the sodium chloride solution and the mixture of hydrogen peroxide and sulfuric acid were controlled and measured by peristaltic pumps. The cell was tested at the temperatures of 25, 40, 50, and 60 °C, respectively. The test temperature was controlled by putting the

Table 1
Electrochemical parameters calculated from polarization tests.

Sample	i_{corr} (A cm^{-2})	E_{corr} (V)	b_c (mV dec^{-1})
Nickel foam	5.4586×10^{-4}	−0.115	−695.05
Silver coated nickel foam	3.3493×10^{-4}	−0.239	−185.01
Titanium foam	3.7568×10^{-7}	0.147	−106.78
Palladium coated nickel foam	4.5736×10^{-5}	0.406	−155.89

testing cell in a thermostatic water bath. The magnesium anode was replaced as an individual test finished.

3. Results and discussion

3.1. Identification of the substrate for the cathode catalysts of the Mg–H_2O_2 fuel cell

To study the electrochemical corrosion behaviors of the nickel foam, the silver coated nickel foam, the titanium foam and the palladium coated titanium foam, polarization curves were conducted on these substrates in a 0.5 M H_2SO_4 solution. The polarization curves are shown in Fig. 2.

From Fig. 2, the corrosion current densities, corrosion potentials and cathodic branch of the Tafel slopes (b_c) for the nickel foam, silver coated nickel foam, titanium foam and palladium coated titanium foam were calculated by Tafel linear extrapolation, respectively, and listed in Table 1. From Table 1, it can be seen that the corrosion current density of nickel foam is

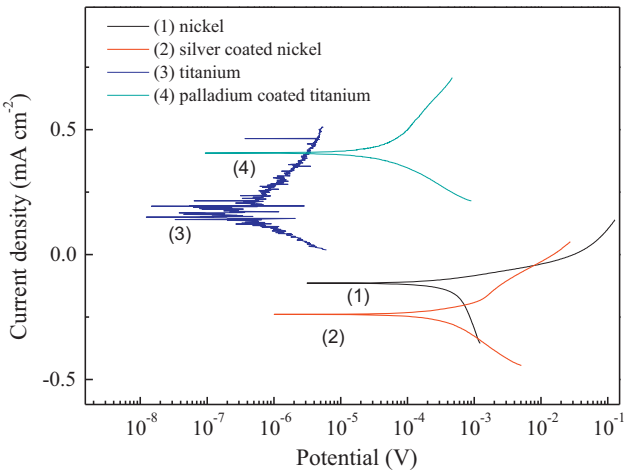

Fig. 2. Polarization curves for the nickel foam, silver coated nickel foam, titanium foam and palladium coated titanium foam in 0.5 M H_2SO_4.

5.4586×10^{-4} A cm^{-2}. After coated by silver, the corrosion current density decreases to 3.3493×10^{-4} A cm^{-2}. In contrast, the corrosion current density of the titanium foam is as low as 3.7568×10^{-7} A cm^{-2}, which is much lower than that for the nickel foam and the silver-coated nickel foam. After coated by palladium, the corrosion current density is 4.5736×10^{-5}, which is still lower than that of nickel and silver coated nickel. From Table 1, we also

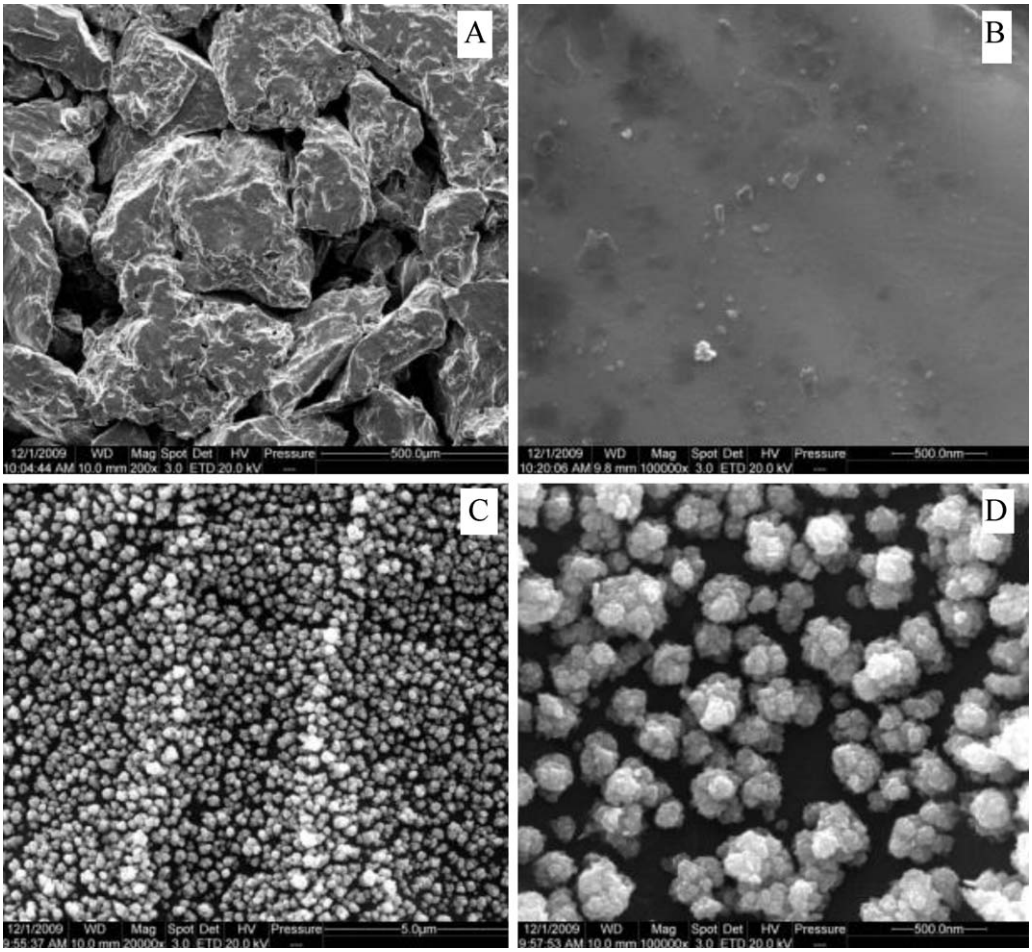

Fig. 3. SEM images of the titanium foam and Pd/Ti foam electrode: (A) titanium foam (low resolution), (B) titanium foam (high resolution), (C) Pd/Ti electrode (low resolution), (D) Pd/Ti electrode surface (high resolution).

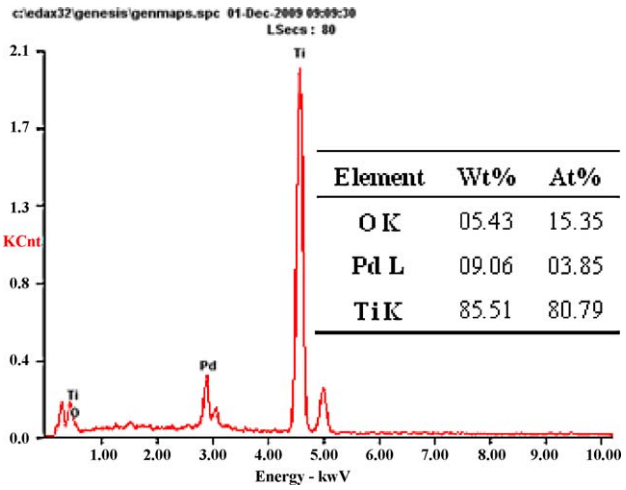

Fig. 4. EDS spectrum of the Pd/Ti electrode.

can see that the onset corrosion potential of the palladium coated titanium foam is the most positive among the four materials. These results indicate that titanium foam was more corrosion-resistant than nickel foam and silver coated nickel foam in acidic media and the palladium coated titanium foam is a potential candidate as a cathode for Mg–H_2O_2 fuel cells.

3.2. Physical properties of the Pd/Ti electrode

Fig. 3 shows the SEM images of the substrate titanium foam (A and B, different resolutions) and the Pd/Ti electrode (C and D, different resolutions) prepared by electrodepositing Pd nanoparticles onto the surface of the titanium foam. It can be seen from Fig. 3A and B that the titanium substrate is porous on a micrometer scale. After deposition of Pd (Fig. 3C and D), the Pd particles distribute uniformly on the substrate with an average particle size of about 100 nm. From Fig. 3D, it can be seen that the large Pd particles of around 100 nm are an aggregation of small primary particles of around 13 nm.

The composition of the Pd/Ti electrode was determined by the EDS analysis, as shown in Fig. 4. Both Pd and Ti are found in the sample and the average content of the Pd is 9.06 wt%.

To investigate the crystal structure of the titanium foam and the Pd/Ti electrode, the XRD patterns of both samples are shown in Fig. 5. To see clearly, the standard patterns of Pd (PCPDF #050681) and Ti (PCPDF#441294) are also included in Fig. 5. For the titanium foam, the peaks centered at around 35°, 38°, 40°, 53°, 63°, 70°, 74°, 76°, 77°, 82°, 86° should be attributed to the diffraction from Ti(1 0 0), Ti(0 0 2), Ti(1 0 1), Ti(1 0 2), Ti(1 1 0), Ti(1 0 3), Ti(2 0 0), Ti(1 1 2), Ti(2 0 1), Ti(0 0 4), Ti(2 0 2) facet, respectively, according to the standard pattern of Ti (PCPDF#441294). For the Pd coated titanium, the peaks at around 40°, 46°, 68°, 82° and 86° are attributed to the diffraction from Pd(1 1 1), Pd(2 0 0), Pd(2 2 0), Pd(3 1 1), Pd(2 2 2) facet, respectively. The average Pd crystal size is about 13 nm calculated using Scherrer's equation based on peak Pd(2 0 0) rather than the main peak Pd(1 1 1), since the main one is overlapped with the peak from Ti(1 0 1) at around 40°. This result is agreeable with the statistic result obtained from the SEM images.

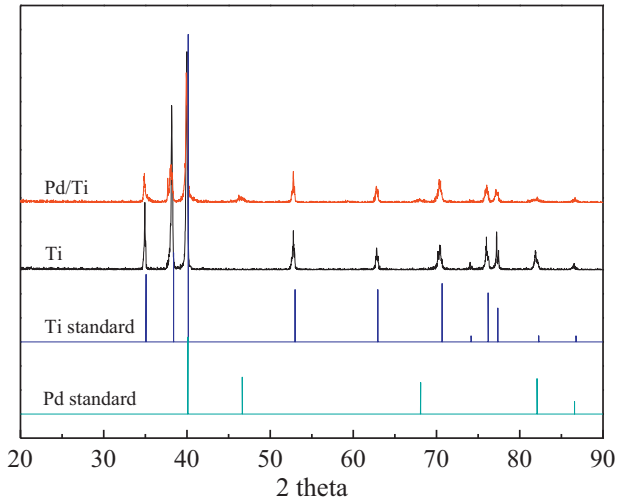

Fig. 5. XRD patterns of Ti foam and Pd/Ti electrode.

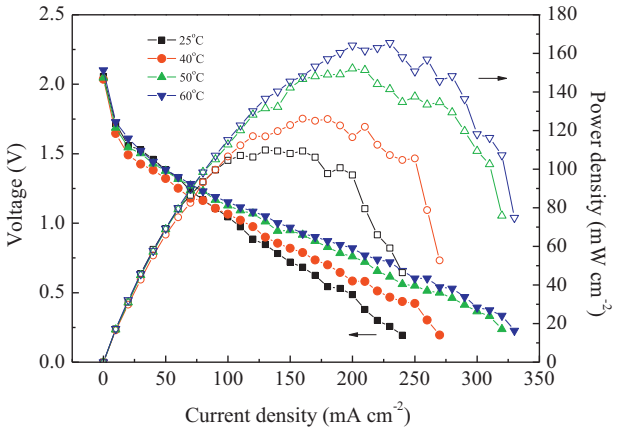

Fig. 6. Performance of the Mg–H_2O_2 fuel cell at different temperatures. Anode: AZ61 magnesium alloy, cathode: Pd/Ti, electrolyte: 40 g L^{-1} NaCl, 100 mL min^{-1}, catholyte: 0.5 M H_2O_2, 0.5 M H_2SO_4, 100 mL min^{-1}.

3.3. The effects of operation conditions on Mg–H_2O_2 fuel cell performances

The polarization curves and power density of Mg–H_2O_2 fuel cell at different operating temperatures ranging from 25 to 60 °C are shown in Fig. 6. It can be seen from the figure that the cell performance increases with the operation temperatures. The peak power density is 110 mW cm^{-2} at 25 °C, and increases to about 168 mW cm^{-2} at 60 °C. The improvement of the cell performance with increasing the operation temperature is mainly attributed to (i) a faster kinetics of both the magnesium electro-oxidation and hydrogen peroxide electro-reduction and (ii) an accelerated ion migration between the anode and the cathode.

It should be mentioned that besides the direct electrochemical reduction of hydrogen peroxide, the decomposition of hydrogen peroxide also occurs at the cathode. The decomposition reaction of hydrogen peroxide could be expressed by Eq. (4).

$$2H_2O_2 \rightarrow 2H_2O + O_2 \quad (4)$$

The electrochemical and decomposition efficiencies of hydrogen peroxide were further studied at different temperatures. The definitions of the electrochemical and decomposition efficiencies are based upon the mass of hydrogen peroxide consumed in the electrochemical and decomposition reactions relative to the total consumed hydrogen peroxide in mass. The total consumed hydrogen peroxide in mass is determined by the $KMnO_4$ titration of the hydrogen peroxide ($5H_2O_2 + 2MnO^{4-} + 6H^+ \rightarrow 2Mn^{2+} + 5O_2\uparrow + 8H_2O$), using $KMnO_4$ itself as the visual indicator at the start and end of the experiment, as described in Ref. [19]. The electrochemical efficiency of hydrogen peroxide can be determined by the integration of the

Table 2
The efficiencies of hydrogen peroxide for the Mg–H_2O_2 fuel cell at different temperatures.

Temperature (°C)	Electrochemical efficiency (%)	Decomposition efficiency (%)
25	77.2	22.8
40	78.5	21.5
50	75.7	24.3
60	73.7	26.3

discharge current over the testing time. The decomposition efficiency of hydrogen peroxide can be obtained by subtracting the percent of the hydrogen peroxide electrochemical efficiency from 100%.

The electrochemical efficiency and decomposition efficiency of hydrogen peroxide in the Mg–H_2O_2 fuel cell at different temperatures are summarized in Table 2.

From Table 2, we find that the electrochemical efficiency of hydrogen peroxide nearly independent of temperature. It should be referred here both the rate of electrochemical reduction reaction and decomposition reaction of hydrogen peroxide increase as increasing temperatures. The former helps to promote but the latter lowers the electrochemical efficiency of hydrogen peroxide. As a result, the electrochemical efficiency of hydrogen peroxide fluctuates in a small range as increasing temperatures.

The effect of hydrogen peroxide concentrations on the cell performance is shown in Fig. 7. The cell performance is improved as the hydrogen peroxide concentration increased. However, as the concentration of hydrogen peroxide increased, the decomposition reaction of hydrogen peroxide is more significant, which produced a lot of gas bubbles that could hinder the mass transfer of the reactants. This explains why the discharge curve in the mass transportation region become fluctuant as the hydrogen peroxide concentration increased.

The electrochemical efficiency and decomposition efficiency of hydrogen peroxide in the Mg–H_2O_2 fuel cell at different hydrogen peroxide concentrations at 25 °C are summarized in Table 3.

From these results it can be found that as the hydrogen peroxide concentration increases, the electrochemical efficiency of hydrogen peroxide decreases. This is because that the decomposition reaction of hydrogen peroxide was a first order reaction [19]. The decomposition rate of hydrogen peroxide was directly proportional to the concentration of hydrogen peroxide.

To investigate the effect of sulfuric acid concentration on the cell performance, different sulfuric acid concentrations including

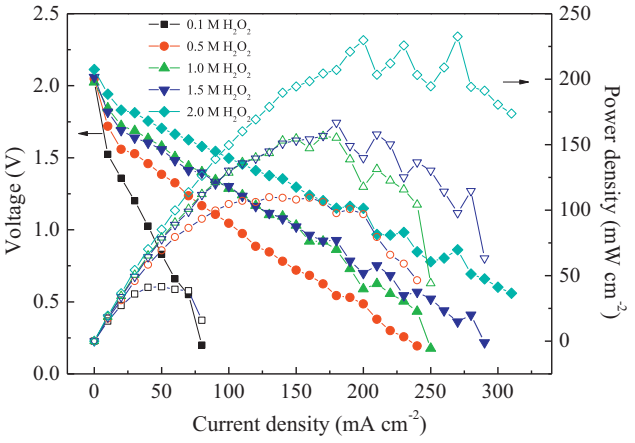

Fig. 7. Comparison of the Mg–H_2O_2 fuel cell performances at different concentrations of hydrogen peroxide. Anode: AZ61 magnesium alloy, cathode: Pd/Ti, Anolyte: 40 g L^{-1} NaCl, 100 mL min^{-1}, catholyte: H_2O_2 + 0.5 M H_2SO_4, 100 mL min^{-1}.

Table 3
The efficiencies of hydrogen peroxide for the Mg–H_2O_2 fuel cell at different hydrogen peroxide concentrations.

$C_{H_2O_2}$ (mol L^{-1})	Electrochemical efficiency (%)	Decomposition efficiency (%)
0.1	88.4	11.6
0.5	77.2	22.8
1.0	59.5	40.5
1.5	47.7	52.3
2.0	40.0	60.0

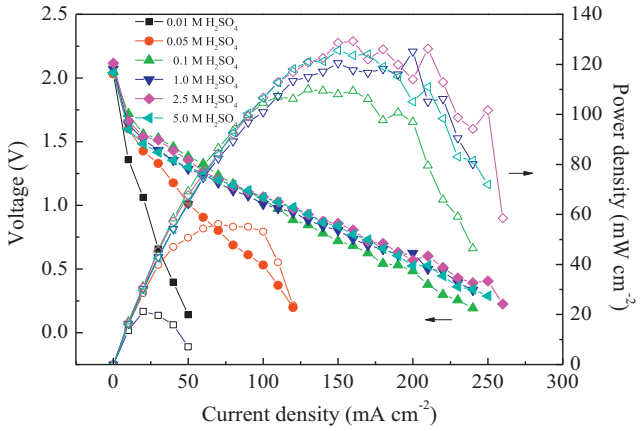

Fig. 8. Performance comparison of Mg–H_2O_2 fuel cells fed with different concentrations of hydrogen peroxide. Anode: AZ61 magnesium alloy, cathode: Pd/Ti, anolyte: 40 g L^{-1} NaCl, 100 mL min^{-1}, catholyte: 0.5 M H_2O_2 + H_2SO_4, 100 mL min^{-1}.

0.01, 0.1, 1.0, 2.5, 5.0 M were fed, respectively, while keeping the hydrogen peroxide concentration at 0.5 M. The cell performances with different sulfuric acid concentrations are shown in Fig. 8. With the concentration of sulfuric acid increased from 0.01 to 1.0 M, the output power density increase obviously, while further increasing the sulfuric acid concentration from 1.0 to 5.0 M did not result in further increase of the output power density. To understand the underlying cause, the electrochemical efficiency of hydrogen peroxide at different sulfuric acid concentrations were calculated and shown in Table 4. From Table 4, it can be seen clearly that the electrochemical efficiency of hydrogen peroxide increased significantly from 3.8 to 72.7% with the sulfuric acid concentration increasing from 0.01 to 1.0 M, while further increasing the sulfuric acid concentration to 5 M results to a slight decrease of the electrochemical efficiency of hydrogen peroxide to 60.0%. This is reasonable since the electrochemical reaction of hydrogen peroxide involves H^+ as a reactant as expressed in Eq. (2). With lower sulfuric acid concentrations (e.g., <1 M) the formation of H^+ in solution is the rate-determining step for the electrochemical reaction of hydrogen peroxide, in other words, the electrochemical reaction of hydrogen peroxide was restrained. As a result, the chemical decomposition of hydrogen peroxide was prevalent, which leads to the lower electrochemical efficiency of hydrogen peroxide with lower sulfuric acid concentrations and the worse fuel cell performance.

Table 4
The efficiencies of hydrogen peroxide for the Mg–H_2O_2 fuel cell at different sulfuric acid concentrations.

$C_{H_2SO_4}$ (mol L^{-1})	Electrochemical efficiency (%)	Decomposition efficiency (%)
0.01	3.8	96.2
0.1	35.9	64.1
1.0	72.7	27.3
2.5	69.2	30.8
5.0	60.0	40.0

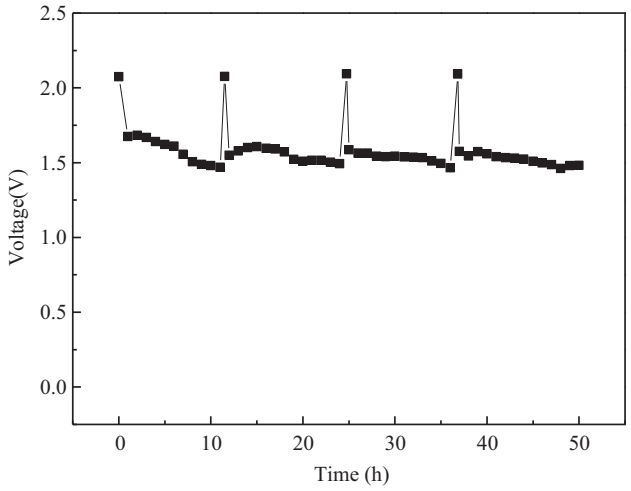

Fig. 9. Stability test of the Mg–H_2O_2 fuel cell with the Pd/Ti as the cathode. Temperature: 20 °C, current density: 25 mA cm^{-2}, anode: AZ61 magnesium alloy, cathode: Pd/Ti, anolyte: 4 wt% NaCl, 100 mL min^{-1}, catholyte: 0.5 M H_2O_2, 0.1 M H_2SO_4,100 mL min^{-1}.

With increasing the sulfuric acid concentration (proton concentration) from 0.01 to 1.0 M, the electrochemical efficiency of hydrogen peroxide increased as reported in Ref. [20], as a result, the cell performance was improved. In addition, it should be mentioned that the proton conductivity of the acidic hydrogen peroxide solution also contributes to the improved cell performance. However, further increasing the sulfuric acid concentration to higher than 1 M, the electrochemical reaction of hydrogen peroxide decreases slightly, thus, the cell performance keeps almost unchanged even though the conductivity of the acidic hydrogen peroxide solution increases. Further studies need to be undertaken to understand this complex effect from sulfuric acid.

The electrochemical and decomposition efficiencies of hydrogen peroxide were calculated employing different concentrations of sulfuric acid. The results are summarized in Table 4.

3.4. Stability of the Mg–H_2O_2 fuel cell

A long duration discharge of the Mg–H_2O_2 fuel cell was conducted to evaluate the stability at room temperature in Fig. 9 of the discharge current was controlled at 25 mA cm^{-2}. Limited by the thickness of magnesium anode, the magnesium anode was replaced about every 10 h. The electrolyte was replaced about every 10 h as well. The result shows that the electrode is relatively stable over the entire test duration of 50 h under constant current of 25 mA cm^{-2} at room temperature.

4. Conclusions

In this work, a nanostructured-Pd coated titanium cathode for the Mg–H_2O_2 fuel cell was fabricated by the electrodeposition method. SEM showed that Pd is formed as spherical clusters on the titanium surface. The Mg–H_2O_2 fuel cell with the Pd/Ti as the cathode presents a higher power density of 110 mW cm^{-2} than that with the Pd–Ag/Ni as the cathode (80 mW cm^{-2}) at 25 °C [13]. A 50 h stability test shows that the nanostructured Pd coated titanium foam cathode is stable under the working conditions of the Mg–H_2O_2 fuel cell, which is a potential cathode candidate for the Mg–H_2O_2 fuel cells.

Acknowledgments

This work is financially supported by National Basic Research Program of China (2012CB215500) and the External Cooperation Program of the Chinese Academy of Sciences (Grant No. GJHZ1135).

References

[1] D.S. Hondt, D.C. Smith, A.J. Spivack, Joides Journal 28 (1) (2002) 51–54.
[2] H.S. Pettingill, P. Weimer, The Leading Edge 21 (4) (2002) 371–376.
[3] V.E. Khaiv, I.D. Polakova, Lithology and Mineral Resources 9 (6) (2004) 610–621.
[4] M.G. Medeiros, R.R. Bessette, C.M. Deschenes, D.W. Atwater, Journal of Power Sources 96 (2001) 236–239.
[5] R.R. Bessette, M.G. Medeiros, C.J. Patrissi, C.M. Deschenes, C.N. LaFratta, Journal of Power Sources 96 (2001) 240–244.
[6] M.G. Medeiros, R.R. Bessette, C.M. Deschenes, C.J. Patrissi, L.G. Carreiro, S.P. Tucker, D.W. Atwater, Journal of Power Sources 136 (2004) 226–231.
[7] W.Q. Yang, S.H. Yang, W. Sun, G.Q. Sun, Q. Xin, Journal of Power Sources 160 (2006) 1420–1424.
[8] L.M. Sun, D.X. Cao, G.L. Wang, Journal of Applied Electrochemistry 38 (2008) 1415–1419.
[9] D.X. Cao, J.D. Chao, L.M. Sun, G.L. Wang, Journal of Power Sources 179 (2008) 87–91.
[10] R.R. Bessette, J.M. Cichon, D.W. Dischert, E.G. Dow, Journal of Power Sources 80 (1999) 248.
[11] C.J. Patrissi, R.R. Bessette, Y.K. Kim, C.R. Schumacher, Journal of the Electrochemical Society 155 (2008) B558–B562.
[12] M.G. Medeiros, E.G. Dow, Journal of Power Sources 80 (1999) 78–82.
[13] W.Q. Yang, S.H. Yang, W. Sun, G.Q. Sun, Q. Xin, Electrochimica Acta 52 (2006) 9–14.
[14] I.M. Khaled, F.M. Ahlam, B.A. Waheed, Corrosion Science 48 (2006) 1912–1925.
[15] J. Zhang, G.P. Yin, Z.B. Wang, Y.Y. Shao, Journal of Power Sources 160 (2006) 1035–1040.
[16] T. Oe, T. Iwamori, A. Suzuki, H. Daimon, K. Fujie, Corrosion 63 (2007) 793–798.
[17] A.V. Sergueeva, V.V. Stolyarov, R.Z. Valiev, A.K. Mukherjee, Scripta Materialia 45 (2001) 747–752.
[18] K.D. Maglic, D.Z. Pavicic, International Journal of Thermophysics 22 (2001) 1833–1841.
[19] L. Shi, A. Goldbach, G.F. Zeng, H.Y. Xu, Journal of Membrane Science 348 (2010) 160–166.
[20] V.R. Choudhary, C. Samanta, T.V. Choudhary, Journal of Molecular Catalysis A: Chemical 260 (2006) 115–120.